
Geometric Knowledge Distillation: Topology Compression for Graph Neural Networks

Chenxiao Yang, Qitian Wu, Junchi Yan*
 Department of Computer Science and Engineering
 MoE Key Lab of Artificial Intelligence
 Shanghai Jiao Tong University
 {chr26195,echo740,yanjunchi}@sjtu.edu.cn

Abstract

We study a new paradigm of knowledge transfer that aims at encoding graph topological information into graph neural networks (GNNs) by distilling knowledge from a teacher GNN model trained on a complete graph to a student GNN model operating on a smaller or sparser graph. To this end, we revisit the connection between thermodynamics and the behavior of GNN, based on which we propose Neural Heat Kernel (NHK) to encapsulate the geometric property of the underlying manifold concerning the architecture of GNNs. A fundamental and principled solution is derived by aligning NHKs on teacher and student models, dubbed as Geometric Knowledge Distillation. We develop non-parametric and parametric instantiations and demonstrate their efficacy in various experimental settings for knowledge distillation regarding different types of privileged topological information and teacher-student schemes.

1 Introduction

Modern graph neural networks (GNNs) [28; 49; 53] have shown remarkable performance in learning representations for structured instances. From the perspective of geometric deep learning [5; 4; 38], part of the achievement of GNNs can be attributed to their implementation of the permutation invariance property as *geometric priors*² into the architecture design. Nevertheless, in practice, GNNs highly rely on graph topology, as essential input information, to explore the relational knowledge implicit in interactions of instance pairs throughout the entire message passing process, termed as *geometric knowledge* in this paper. As advances in generalized distillation [33; 47] reveal the possibility of encoding input features into model construction, natural questions arise as to:

Is it possible, and if so, how can we encode graph topology as a special type of ‘geometric prior’ into a GNN model, such that the model could precisely capture the underlying geometric knowledge even without full graph topology as input?

In specific, we are interested in the following *geometric knowledge transfer* problem: a GNN model (with node-specific outputs for node-level prediction [23]) is exposed with a partial graph, which is a subset of the complete graph. Formally speaking, we have notations:

$$\mathcal{G} = \{\mathcal{V}, \mathcal{E}\} \text{ (partial graph)}, \tilde{\mathcal{G}} = \{\tilde{\mathcal{V}}, \tilde{\mathcal{E}}\} \text{ (complete graph)}, \text{ where } \mathcal{V} \subseteq \tilde{\mathcal{V}}, \mathcal{E} \subseteq \{\mathcal{V} \times \mathcal{V}\} \cap \tilde{\mathcal{E}}. \quad (1)$$

Our goal is to transfer or encode geometric knowledge extracted from $\tilde{\mathcal{G}}$ to the target GNN model that is only aware of \mathcal{G} . Studying this problem is also of much practical value. As a non-exhaustive

*Junchi Yan is the correspondence author who is also with Shanghai AI Laboratory.

²Geometric priors originally refer to the geometric principles naturally encoded in deep learning architectures, e.g., translational symmetry for CNNs, permutation invariance for GNNs.

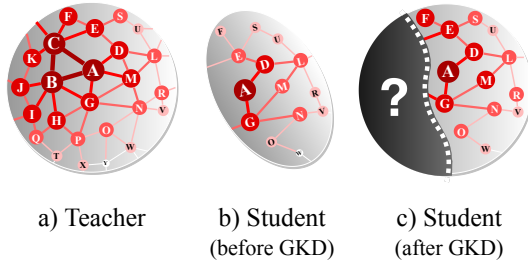


Figure 1: Feature propagation on the underlying manifold \mathcal{M} . (a) Teacher: aware of the complete graph topology, and faithfully explore geometric knowledge about the underlying manifold. (b) Student before GKD: only aware of partial graph topology, and estimate biased geometry property. (c) Student after GKD: able to propagate features on the same space as teacher by alignment of NHKs.

list of applications: improving efficiency without compromising on effectiveness for coarsened graphs [14; 24; 69], privacy constrained scenarios in social recommenders or federated learning where the complete graph is unavailable [34; 50; 68], promoting concentration on targeted community to bring up economic benefits [57].

Achieving this target is non-trivial for that we need to first find a principled and fundamental way to encapsulate the geometric knowledge extracted by GNN model, which requires in-depth investigation on the role of graph topology throughout the progressive process of message passing. Therefore, we take a thermodynamic view borrowed from physics and propose a new methodology built upon recent advances revealing the connection between heat diffusion and architectures of GNNs [8; 51; 7]. Specifically, we interpret feature propagation as heat flows on the underlying Riemmanian manifold, whose characteristics (that are dependent on graph topology and the GNN model) pave the way for a principled representation of the latent geometric knowledge.

1.1 Our Contributions

New theoretical perspective for analyzing latent graph geometry. On top of the connection between heat equation and GNNs, we step further to inspect the implication of heat kernel for GNNs, and propose a novel notion of *Neural Heat Kernel* (NHK) with rigorous proof of its existence. Heat kernel intrinsically defines the unique solution to the heat equation and can be a fundamental characterization for the geometric property of the underlying manifold [18; 19]. Likewise, NHK uncovers geometric property of the latent graph manifold for GNNs, and governs how information flows between pairs of instances, which lends us a mathematical tool to encapsulate geometric knowledge extracted from GNN model and enables geometric knowledge transfer. This result alone might also be useful in broader contexts for understanding GNNs.

Flexible distillation framework with versatile instantiations. Based on the above insights, we treat NHK matrices as representation of the latent geometric knowledge, upon which we build a flexible and principled distillation framework dubbed as *Geometric Knowledge Distillation* (GKD), which aims at encoding and transferring geometric knowledge by aligning latent manifolds behind GNN models as illustrated in Fig. 1. We also develop non-parametric and parametric versions of GKD, in terms of different ways to approximate NHK computation. Specifically, the former derives explicit NHKs via assumptions on latent space, and the later learns NHK in a data-driven manner.

Applications for geometric knowledge transfer and conventional KD purposes. We verify the efficacy of GKD in terms of different geometric knowledge types (i.e., edge-aware and node-aware ones), and further show its effectiveness for conventional KD purposes (e.g., model compression, self distillation, online distillation) for broader applicability. We highlight that our methods consistently exceed teacher model and rival with the oracle model that gives the performance upper bound in principle.

1.2 Links to Related Works

Geometric Deep Learning. The study of geometric deep learning [5; 38] provides fundamental principles and methodology to generalize deep learning methods to non-Euclidean domains (e.g., graphs and manifolds). From this perspective, architectures for off-the-shelf GNNs [28; 49; 53; 20] and graph Transformers [67; 56] have naturally incorporated the geometric prior knowledge for graphs such as *permutation invariance*. Despite their remarkable success, they highly rely on the graph topology. This work extends the idea of geometric deep learning by treating the global graph

topology as a special type of prior knowledge, and attempts to encode it into GNNs themselves, such that the trained model would leverage information from the global graph topology even without explicitly taking it as input.

Graph-Based Knowledge Distillation. Knowledge distillation (KD) [22; 1] uses the outputs of a teacher model as alternative supervised signals to teach a student model, with various new paradigms including feature-based [42; 66] and relation-based [64; 65] ones. While some prior arts [9; 61; 50; 69; 63; 60] attempted to combine KD and GNNs, i.e., graph-based KD, they are nearly straight-forward adaptations of KD without in-depth investigation on the role of graph topology, also restricted by a specific choice of GNN architecture or application scenarios. In contrast, we first formalize the problem of geometric knowledge transfer, theoretically answer the question “how to represent graph geometric knowledge and encode it into GNN models”, and propose geometric distillation approach based on the theoretical results. More discussions on related works are deferred to Appendix G.

2 Preliminaries

We commence with a brief detour to heat equation on Riemannian manifolds, and its connection with modern GNN architectures. Moreover, we bring forth the notion of *heat kernel* to motivate this work.

Heat Equation on Manifolds. We are interested in heat equation defined on a smooth k -dimensional Riemannian manifold \mathcal{M} . Suppose the manifold is associated with a scalar- or vector-valued function $x(u, t) : \mathcal{M} \times [0, \infty) \rightarrow \mathbb{R}^d$, quantifying a specific type of signals such as *heat* at a point $u \in \mathcal{M}$ and time t . Fourier’s law of heat conductivity describes the flow of heat with respect to time and space, via a partial differential equation (PDE) called *heat equation* [6], i.e.,

$$\frac{\partial x(u, t)}{\partial t} = -c \Delta x(u, t), \quad (2)$$

where $c > 0$ is the *thermal conductivity* coefficient, and Δ is the natural *Laplace–Beltrami operator* associated with \mathcal{M} . Rewriting Δ as the functional composition of the *divergence operator* ∇^* and *gradient operator* ∇ , i.e., $\Delta = \nabla^* \circ \nabla$, we can interpret the heat equation as: the variation of temperature within an infinitesimal time interval at a point is equivalent to the divergence between its own temperature and the average temperature on an infinitesimal sphere around it.

Implications on Graphs. A spatial discretisation of a continuous manifold yields a graph $\mathcal{G} = \{\mathcal{V}, \mathcal{E}\}$, whose nodes can be thought of as embedded on the base manifold. In fact, the heat equation along with variants thereof (e.g., Schrödinger equation) have found widespread use in modeling graph dynamics [11; 25; 36]. More importantly, it has been recently revealed to be intimately related with the architectures of modern GNNs [51; 8; 7]: suppose $\mathbf{X}(0) = \{x(u, 0)\}_{u \in \mathcal{V}} \in \mathbb{R}^{n \times d}$ denotes the initial condition for Eqn. (2) determined by input node features, then solving the heat equation under certain definitions of ∇^* and ∇ (i.e., definition of Δ) amounts to different architectures of GNNs. For instance:

Example 1. [51] Define the discretised counterpart of Δ as the graph Laplacian matrix $\mathbf{L} = \tilde{\mathbf{D}}^{-\frac{1}{2}}(\tilde{\mathbf{D}} - \tilde{\mathbf{A}})\tilde{\mathbf{D}}^{-\frac{1}{2}}$. Numerically solving Eqn. (2) using the forward Euler method with step size $\tau = 1$ yields the formulation of Simple Graph Convolution (SGC) [53], where Θ denote learnable transformation matrix

$$\hat{\mathbf{X}}(t) = \left(\tilde{\mathbf{D}}^{-\frac{1}{2}}\tilde{\mathbf{A}}\tilde{\mathbf{D}}^{-\frac{1}{2}}\right)^t \mathbf{X}(0), \quad \hat{\mathbf{Y}} = \text{softmax}\left(\hat{\mathbf{X}}(t)\Theta\right). \quad (3)$$

Example 2. [8] Define the gradient operator ∇_{ij} as the difference of source and target node features, the divergence operator ∇_i^* as the sum of features of all edges for the node. Numerically solving Eqn. (2) using the explicit Euler scheme with step size τ yields the following recursive formulation

$$\hat{\mathbf{X}}(t + \tau) = \tau(\mathbf{G} - I)\hat{\mathbf{X}}(t) + \hat{\mathbf{X}}(t) \quad (4)$$

where \mathbf{G} is a diffusivity coefficient matrix in place of c .

Moreover, stacking a non-linear transformation layer after each step yields the formulation of Graph Convolution Networks (GCN) [28] for Eqn. (3), Graph Attention Networks (GAT) [49] with residual connection for Eqn. (4), and even more GNN architectures by virtue of the flexibility of interpretation for heat equation on graphs.

Heat Kernels. Intriguingly, it turns out that the initial value problem of heat equation on any manifold \mathcal{M} has a smallest positive fundamental solution depending on the Laplace operator Δ , known as the *heat kernel* [2]. It is denoted as a kernel function $\kappa(x, y, t)$, such that

$$x(u_i, t) = e^{-t\Delta}x(u_i, 0) = \int_{\mathcal{M}} \kappa(u_i, u_j, t)x(u_j, 0)d\mu(u_j), \quad (5)$$

where μ is a non-negative measure associated with \mathcal{M} . In physics, the heat kernel $\kappa(x, y, t)$ can be interpreted as a transition density that describes the asymptotic behavior of a natural Brownian motion on the manifold. Its formulation thus can be treated as *a unique reflection or representation of the geometry of the underlying manifold*. For example, if the manifold is a *k-dimensional Euclidean Space* \mathbb{R}^k or a *Hyperbolic Space* \mathbb{H}^k , the explicit formula of heat kernel is respectively given by,

$$\kappa(u_i, u_j, t) = \frac{1}{(4\pi t)^{k/2}} \exp\left(-\frac{\rho^2}{4t}\right) \text{ and } \kappa(u_i, u_j, t) = \frac{(-1)^m}{2^m \pi^m} \frac{1}{(4\pi t)^{\frac{1}{2}}} \left(\frac{1}{\sinh \rho} \frac{\partial}{\partial \rho}\right)^m e^{-m^2 t - \frac{\rho^2}{4t}}, \quad (6)$$

where $\rho = d(u_i, u_j)$ denote geodesic distance. Heat kernel has also been adopted for graph-related applications such as community detection [31], graph clustering [58].

3 Extending Heat Kernel to GNNs

The starting point of this work is the development of *neural heat kernel*, built upon the previously-mentioned connection of GNNs and heat equation. As will be discussed later, this novel notion lends us a thermodynamic perspective to the intrinsic geometric property of the latent graph manifold embodied in GNNs, and hence paves the way for distilling geometric knowledge.

3.1 Neural Heat Kernel

Consider the graph signal $\mathbf{X}(t)$ at time t and node features $\mathbf{H}^{(l)}$ at layer l as interchangeable notions. Consequently, feature propagation using one layer of GNN amounts to heat diffusion on the base manifold \mathcal{M} within a certain time interval τ , leading to the equivalences of $\mathbf{X}(t + \tau)$ and $\mathbf{H}^{(l+1)}$:

$$\mathbf{H}^{(l+1)} = f_\theta(\mathbf{H}^{(l)}, \mathcal{G}), \quad \mathbf{X}(t + \tau) = e^{-\tau\Delta(f_\theta, \mathcal{G})}\mathbf{X}(t), \quad (7)$$

where f_θ denotes an arbitrary GNN model with parameter θ , and $\Delta(f_\theta, \mathcal{G})$ denotes a generalization of Laplace-Beltrami operator defined over the base manifold \mathcal{M} associated with graph \mathcal{G} and the arbitrary backbone GNN model f_θ .

Remark. The equivalence of two equations in Eqn. 7 is based on the recently established connection between heat equation and GNNs [8; 7; 51; 13; 12], which reveal that the formulation of a GNN layer could be thought of as discretisations (that correspond to the left equation in Eqn. 7) of the continuous diffusion process (that correspond to the right equation in Eqn. 7) described by the heat equation. Furthermore, different definitions of Laplace-Beltrami operator Δ and schemes for solving Eqn. 2 could yield different GNNs (e.g., SGC [53], GAT [49], GRAND [8]). While it is unclear whether there exists such a definition of Δ for every GNN architecture, we write the operator as $\Delta(f_\theta, \mathcal{G})$ to associate it with model f_θ , and then use the analogy between GNN and heat equation as an analytical tool, in a similar manner with [3; 46; 51; 45; 8; 7], for studying the geometry property of GNNs. See more detailed justifications in Appendix E.

In light of this connection, we consider a natural generalization of heat kernel for GNNs, termed as *neural heat kernel (NHK)* to highlight its difference with heat kernel in the thermodynamic context. In particular, a *single-layer NHK* is defined as a positive definite symmetric kernel function denoted as $\kappa_\theta^{(l)}(v_i, v_j)$, where the sub-script θ implies that it is associated with the architecture and parameters of the backbone GNN, and the super-script (l) implies that it is specific to each layer, analogous to the role of continuous time t in Eqn. (5).

Theorem 1. (Existence of Single-Layer NHK) *Suppose two expressions in Eqn. (7) are equivalent (see Appendix E for more discussions), then for any graph \mathcal{G} and GNN model f_θ , there exist a unique single-layer NHK function $\kappa_\theta^{(l)}(\cdot)$ such that for any node $v_i \in \mathcal{V}$ and $l > 0$,*

$$\mathbf{h}_i^{(l)} = \sum_{v_j \in \mathcal{V}} \kappa_\theta^{(l)}(v_i, v_j) \cdot \mathbf{h}_j^{(l-1)} \mu(v_j) \quad (8)$$

where $\mathbf{h}_i^{(l)} \in \mathbb{R}^d$ denotes the feature of node v_i at l -th layer, and μ is a measure over vertices that could be specified as the inverse of node degree $1/d_i$.

To push further, we can generalize NHK across multiple layers of GNN, termed as a *cross-layer NHK* $\kappa_\theta(v_i, v_j, l \mapsto l+k)$ (e.g., from l -th layer to $(l+k)$ -th layer of GNN). Its existence could be induced recursively by the *semi-group identity property* of NHK concerning consecutive GNN layers.

Theorem 2. (Semigroup Identity Property of NHK) *The NHK satisfies the semigroup identity property: $\forall v_i, v_j \in \mathcal{V}$ and $l > 0$, there exists a cross-layer NHK across two consecutive layers*

$$\kappa_\theta(v_i, v_j, l \mapsto l+2) = \sum_{v_k \in \mathcal{V}} \kappa_\theta^{(l+1)}(v_i, v_k) \kappa_\theta^{(l+2)}(v_k, v_j) d\mu(v_k) \quad (9)$$

This theorem indicates that stacks of multiple GNN layers also constitute a valid kernel, i.e.,

$$\mathbf{h}_i^{(l+k)} = \sum_{v_j \in \mathcal{V}} \kappa_\theta(v_i, v_j, l \mapsto l+k) \cdot \mathbf{h}_j^{(l)} \mu(v_j). \quad (10)$$

Analogous to heat kernel as an unique characterization of the underlying space, NHK characterizes the geometric property of the latent graph manifold for GNNs. Additionally, NHK is dependent on GNN models through the definition of the associated Laplace-Beltrami operator $\Delta(f_\theta, \mathcal{G})$, inheriting the expressiveness of neural networks and varying through the course of training. Intuitively, NHK can be thought of as a model-driven encoding for topological information, encapsulating the geometric knowledge learned by GNNs into a tractable functional form.

3.2 Application in Geometric Distillation

Consider the problem of distilling geometric knowledge, which involves an intelligent teacher model f_{θ^*} , which is exposed to and pre-trained over the (relatively) *complete graph* $\tilde{\mathcal{G}} = (\tilde{\mathcal{V}}, \tilde{\mathcal{E}})$, and a student model f_θ that is exposed to the partial graph $\mathcal{G} = (\mathcal{V}, \mathcal{E})$, where $\mathcal{V} \subseteq \tilde{\mathcal{V}}$ and $\mathcal{E} \subseteq \{\mathcal{V} \times \mathcal{V}\} \cap \tilde{\mathcal{E}}$. Our target is to train a student model (with the help of teacher model) that operates on \mathcal{G} to be as competitive as models operating on $\tilde{\mathcal{G}}$ during inference. Since \mathcal{G} is a sub-graph of $\tilde{\mathcal{G}}$, they should lie in the *same space* (i.e., latent manifold) governed by the underlying mechanism of data generation, and hence we expect student and teacher models to capture the *same geometric property* of this shared space. This leads to the principle of *Geometric Knowledge Distillation* (GKD): transfer the geometric knowledge of the intelligent teacher to the student such that the student can propagate features as if it is aware of the complete graph topology (see the example in Fig. 1).

To this end, we resort to *NHK matrices* on the teacher (resp. student) model over the complete (resp. partial) graph as instantiations of their geometric knowledge, denoted as

$$\begin{aligned} \text{(Teacher)} \quad \mathbf{K}_{\theta^*}(\tilde{\mathcal{G}}, l \mapsto l+k) &= \{\kappa_{\theta^*}(v_i, v_j, l \mapsto l+k)\}_{|\tilde{\mathcal{V}}| \times |\tilde{\mathcal{V}}|}, \\ \text{(Student)} \quad \mathbf{K}_\theta(\mathcal{G}, l \mapsto l+k) &= \{\kappa_\theta(v_i, v_j, l \mapsto l+k)\}_{|\mathcal{V}| \times |\mathcal{V}|}, \end{aligned}$$

written compactly as $\mathbf{K}^{(l+1)}(\mathcal{G})$ when $k=1$. The NHK matrix is a positive semi-definite symmetric matrix, and alike κ , is dependent on the GNN model f_θ and graph \mathcal{G} . Denote $\mathbf{K}_{\theta^*, \mathcal{V}}^{(l)}(\tilde{\mathcal{G}}) \in \mathbb{R}^{|\mathcal{V}| \times |\mathcal{V}|}$ as the sub-matrix of $\mathbf{K}_{\theta^*}^{(l)}(\tilde{\mathcal{G}})$ with row and column indices in \mathcal{V} . The distillation loss for GKD is

$$\mathcal{L}_{dis}(\mathbf{K}_{\theta^*, \mathcal{V}}, \mathbf{K}_\theta, l \mapsto l+k) = d(\mathbf{K}_{\theta^*, \mathcal{V}}(\tilde{\mathcal{G}}, l \mapsto l+k), \mathbf{K}_\theta(\mathcal{G}, l \mapsto l+k)), \quad (11)$$

where $d(\cdot, \cdot)$ is a similarity measure, for which we choose Frobenius distance as implementation, i.e.,

$$d(\mathbf{K}_{\theta^*, \mathcal{V}}, \mathbf{K}_\theta) = \|(\mathbf{K}_{\theta^*, \mathcal{V}} - \mathbf{K}_\theta) \odot \mathbf{W}\|_{\text{F}}^2, \quad \mathbf{W}_{v_i, v_j} = \begin{cases} 1 & \text{if } (v_i, v_j) \in \mathcal{E} \\ \delta & \text{if } (v_i, v_j) \notin \mathcal{E} \end{cases} \quad (12)$$

where $\mathbf{W} \in \mathbb{R}^{|\mathcal{V}| \times |\mathcal{V}|}$ is a weighting matrix to trade-off distillation loss with respect to different node pairs depending on their connectivity. For $k=1$, the loss can be re-written as $\mathcal{L}_{dis}^{(l+1)}(\mathbf{K}_{\theta^*, \mathcal{V}}, \mathbf{K}_\theta)$. Note that one can also specify different k for teacher and student models in Eqn. (11) in case when the teacher model is deeper.

4 Instantiations for Geometric Knowledge Distillation

Unfortunately, deriving explicit formulas for NHKs is prohibitively challenging due to introduction of non-linearity. To circumvent it, we propose two types of instantiations for GKD, i.e., non-parametric and parametric. The former considers explicit NHKs by making assumptions on the underlying space, and the latter learns NHK in a data-driven manner.

4.1 Non-Parametric Geometric Distillation

Deterministic Kernel. One instantiation of NHK is a *Gauss-Weierstrass kernel* in the form of Eqn. (6), by assuming the underlying space is a Euclidean space. Since the distillation loss in Eqn. (11) is a homogeneous function, we can remove its scaling factor and define NHK as

$$\text{(Gauss-Weierstrass NHK)} \quad \kappa_\theta(v_i, v_j, l \mapsto l + k) \triangleq \exp\left(-\frac{\|\mathbf{h}_i^{(l)} - \mathbf{h}_j^{(l)}\|_2^2}{4T}\right), \quad (13)$$

where T denotes the estimation of the accumulated time interval. Alternatively, we can use *Sigmoid kernel* and define non-parametric NHK as:

$$\text{(Sigmoid NHK)} \quad \kappa_\theta(v_i, v_j, l \mapsto l + k) \triangleq \tanh\left(a \langle \mathbf{h}_i^{(l)}, \mathbf{h}_j^{(l)} \rangle + b\right), \quad (14)$$

where a, b are positive constants depending on l and k . It is a natural and intuitive choice as similarity measurement and empirically found as-well effective, albeit does not correspond to any named manifold to our knowledge.

Randomized Kernel. We can also define *Randomized kernel* based on the following theorem.

Theorem 3. (Expansion of NHK) Let $\{\varphi_{k'}\}_{k'=0}^\infty$ be orthonormal basis of eigenfunctions of $-\Delta(f_\theta, \mathcal{G})$ with eigenvalues $0 < \lambda_0 \leq \lambda_1 \leq \lambda_2 \leq \dots$, NHK allows the expansion:

$$\kappa_\theta(v_i, v_j, l \mapsto l + k) = \sum_{k'=0}^\infty e^{-\lambda_{k'} T} \varphi_{k'}(v_i)^\top \varphi_{k'}(v_j). \quad (15)$$

Based on this result, we resort to the approximation of NHK by defining a randomized kernel in a similar form as Eqn. (15), leading to the following formulation of randomized NHK:

$$\text{(Randomized NHK)} \quad \kappa_\theta(v_i, v_j, l \mapsto l + k) \triangleq \frac{1}{m} \sum_{k'=0}^m e^{-\lambda_{k'} T} \left[\sigma(\mathbf{W}_{k'} \mathbf{h}_i)^\top \sigma(\mathbf{W}_{k'} \mathbf{h}_j) \right], \quad (16)$$

where $\sigma(\mathbf{W}_{k'} \mathbf{h}_i)$ is used to proximate $\varphi_{k'}(v_i)$, $\mathbf{W}_{k'} = [\phi_{1,k'}, \phi_{2,k'}, \dots, \phi_{s,k'}]^\top$ is a transformation matrix, $\phi \sim \mathcal{N}(\mathbf{0}, \mathbf{I}_d)$ is a d -dimensional random variable from Gaussian distribution. In fact, under certain choice of activation function σ , Eqn. (16) could approximate a diversity of kernels [41; 10]. This design essentially enforces the alignment of teacher and student for arbitrary underlying manifold.

Training Scheme. We follow the standard training paradigm in KD literature [22; 17]: the teacher is pre-trained by a supervised prediction loss involving all labeled nodes in $\tilde{\mathcal{V}}$. After teacher is well-trained, we fix θ^* and train the student model according to

$$\theta = \arg \min_{\theta} \mathcal{L}_{pre}(\hat{\mathbf{Y}}_\theta, \mathbf{Y}) + \frac{\alpha}{L} \sum_{l=1}^L \mathcal{L}_{dis}^{(l)}(\mathbf{K}_{\theta^*, \mathcal{V}}, \mathbf{K}_\theta), \quad (17)$$

where \mathbf{Y} denotes ground-truth labels of labeled nodes in \mathcal{V} , and $\hat{\mathbf{Y}}_\theta$ denotes the predictions of student model f_θ on \mathcal{G} , \mathcal{L}_{dis} is the distillation loss defined by Eqn. (11), L denotes the total number of layers.

4.2 Parametric Geometric Distillation

Inheriting the similar spirit of auto-encoding Bayes [27], we introduce a *variational inverse-NHK* that is independently parameterized, denoted as κ_ϕ^\dagger , whose existence is guaranteed by the invertibility of

NHK matrices. Together with κ_θ , they define a symmetric form characterizing feature propagation:

$$\text{(Forward)} \quad \mathbf{h}_i^{(l+k)} = \sum_{v_j \in \mathcal{V}} \kappa_\theta(v_i, v_j, l \mapsto l+k) \cdot \mathbf{h}_j^{(l)} \mu(v_j), \quad (18)$$

$$\text{(Backward)} \quad \mathbf{h}_i^{(l)} = \sum_{v_j \in \mathcal{V}} \kappa_\phi^\dagger(v_i, v_j, l+k \mapsto l) \cdot \mathbf{h}_j^{(l+k)} \mu(v_j). \quad (19)$$

In practice, we follow existing kernel learning approaches [52] and parameterize the inverse-NHK as

$$\kappa_\phi^\dagger(v_i, v_j, l+k \mapsto l) = g_\phi(\mathbf{h}_i^{(l+k)})^\top g_\phi(\mathbf{h}_j^{(l+k)}), \quad (20)$$

where $g_\phi : \mathbb{R}^d \rightarrow \mathbb{R}^s$ is the associated learnable non-linear mapping. Given a pre-trained teacher model, distilling geometric knowledge boils down to 1) establishing equivalence of Eqn. (18) and Eqn. (19), and 2) matching pseudo-inverse NHK matrices for teacher and student models (respectively denoted as $\mathbf{K}_{\theta^*, \mathcal{V}}^\dagger$ and $\mathbf{K}_\theta^\dagger$ with clear meanings), leading to the training scheme as follows.

Training Scheme. Based on Eqn. (19), we can define a *reconstruction loss* with respect to the teacher model (similar applies to the student model) as

$$\mathcal{L}_{rec}(\mathbf{H}_t^{(l+k)}, \mathbf{H}_t^{(l)}) = \|\mathbf{K}_{\theta^*}^\dagger \mathbf{H}_t^{(l+k)} - \mathbf{H}_t^{(l)}\|_F^2. \quad (21)$$

Then, minimizing the reconstruction loss with fixed GNN model parameter θ amounts to optimizing the variational parameter ϕ , and minimizing prediction and distillation losses given fixed ϕ amounts to optimizing the student model parameter θ :

$$\phi \leftarrow \arg \min_{\phi} \quad \mathcal{L}_{rec}(\mathbf{H}_t^{(l+k)}, \mathbf{H}_t^{(l)}) + \mathcal{L}_{rec}(\mathbf{H}^{(l+k)}, \mathbf{H}^{(l)}), \quad (22)$$

$$\theta \leftarrow \arg \min_{\theta} \quad \mathcal{L}_{pre}(\hat{\mathbf{Y}}_\theta, \mathbf{Y}) + \alpha \mathcal{L}_{dis}(\mathbf{K}_{\theta^*, \mathcal{V}}^\dagger, \mathbf{K}_{\theta^*, \mathcal{V}}^\dagger, l+k \mapsto l). \quad (23)$$

Applying two steps iteratively adds up to an EM-like algorithm for training the student model. In practice, we set $l+k$ as the last layer, and l as the first layer to use as much information as possible. We justify the parametric GKD approach in Appendix. D by showing it essentially explores the true NHK behind GNN.

5 Experiments

We conduct experiments to validate the efficacy of our method on graph-structured data in terms of various types of privileged geometric knowledge, combinations of teacher-student GNN architectures and potential application scenarios. We use three benchmark datasets Cora [35], Citeseer [44], Pubmed [39], and a larger dataset OGBN-Arxiv [23] for node classification tasks. More implementation details and experimental results are deferred to Appendix. The codes are available at <https://github.com/chr26195/GKD>.

Implementation and Competitors. We consider the following variants of the proposed GKD. 1) *GKD-G*: non-parametric Gaussian NHK; 2) *GKD-S*: non-parametric Sigmoid NHK; 3) *GKD-R*: randomized NHK; 3) *PGKD*: parametric NHK. We choose KD methods that is representative in its own category for comparison, including *KD* [22], *FSP* [64], *LSP* [63]. We also report the performances of teacher and student model trained with the standard classification loss, short as *Teacher* and *Student*. The teacher model is trained using the complete graph $\tilde{\mathcal{G}}$, and, to calibrate with all other methods, tested using the partial graph \mathcal{G} . Besides, we consider an *Oracle* model which is both trained and tested on $\tilde{\mathcal{G}}$, which naturally takes an advantaged place given more information during inference. Since our method is compatible with the vanilla KD paradigm [22], we report the performance delivered by their combinations (i.e., GKD+KD and PGKD+KD).

Experiment Settings. We investigate on various experimental settings according to different types of privileged geometric knowledge. In the case of *edge-aware geometric knowledge*, the teacher model has access to additional edge information, i.e., $\mathcal{E} \subset \tilde{\mathcal{E}}$ and $\mathcal{V} = \tilde{\mathcal{V}}$. In the case of *node-aware geometric knowledge*, the teacher model has access to additional node information, i.e., $\mathcal{V} \subset \tilde{\mathcal{V}}$ and $\mathcal{E} = \tilde{\mathcal{E}} \cap \{\mathcal{V} \times \mathcal{V}\}$. We also consider other conventional KD settings including model compression, self-distillation and online distillation, which will be illustrated in detail. The backbone f_θ is set as 3-layer GCN [28] for both student and teacher models, unless otherwise stated.

	Cora	CiteSeer	PubMed		Cora	CiteSeer	PubMed
Oracle	88.63 ± 0.48	73.64 ± 0.48	87.16 ± 0.19	Oracle	88.63 ± 0.48	73.64 ± 0.48	87.16 ± 0.19
Teacher	84.61 ± 0.37	70.88 ± 0.62	84.42 ± 0.52	Teacher	87.27 ± 0.51	72.92 ± 0.90	85.98 ± 0.23
Student	83.84 ± 1.32	69.94 ± 0.76	85.35 ± 0.43	Student	84.84 ± 1.61	70.32 ± 1.12	84.74 ± 0.27
KD	84.84 ± 1.19	70.04 ± 0.37	85.58 ± 0.32	KD	86.71 ± 0.77	71.96 ± 1.10	85.55 ± 0.45
FitNets	83.72 ± 1.45	69.99 ± 0.56	85.66 ± 0.27	FitNets	86.09 ± 1.12	72.00 ± 0.78	85.78 ± 0.26
FSP	83.55 ± 2.19	71.43 ± 1.26	85.46 ± 0.34	FSP	85.85 ± 1.66	70.92 ± 1.46	85.20 ± 0.45
LSP	83.99 ± 1.39	70.23 ± 0.79	85.37 ± 0.49	LSP	85.67 ± 1.22	70.66 ± 1.01	85.71 ± 0.50
GKD-G	87.68 ± 1.07	73.04 ± 0.70	85.74 ± 0.38	GKD-G	88.66 ± 0.85	73.18 ± 0.88	86.07 ± 0.45
GKD-S	88.01 ± 0.79	72.46 ± 0.52	85.94 ± 0.43	GKD-S	88.54 ± 0.52	72.85 ± 0.57	86.10 ± 0.42
GKD-R	88.48 ± 0.59	72.97 ± 0.53	86.19 ± 0.55	GKD-R	88.98 ± 0.39	72.80 ± 0.22	86.16 ± 0.33
PGKD	88.41 ± 0.62	73.12 ± 0.58	86.41 ± 0.24	PGKD	89.15 ± 0.45	73.33 ± 0.36	86.09 ± 0.54
GKD+KD	88.95 ± 0.30	73.21 ± 0.53	86.29 ± 0.28	GKD+KD	89.10 ± 0.44	72.94 ± 0.80	86.24 ± 0.26
PGKD+KD	89.09 ± 0.40	73.45 ± 0.48	86.48 ± 0.52	PGKD+KD	89.23 ± 0.61	73.41 ± 0.60	86.20 ± 0.36

Table 1: Results of node classification accuracy for the edge-aware knowledge setting.

Table 2: Results of node classification accuracy for the node-aware setting.

Setting	Oracle	Teacher	Student	KD	GKD	PGKD
Edge-Aware	71.46 ± 0.41	67.96 ± 0.78	66.41 ± 0.45	68.63 ± 1.21	70.90 ± 0.80	71.38 ± 1.01
Node-Aware	71.46 ± 0.41	69.35 ± 0.72	67.49 ± 0.65	68.86 ± 0.66	71.31 ± 0.83	71.27 ± 0.70

Table 3: Results of testing accuracy on OGBN-Arxiv dataset.

5.1 Main Results

Edge-Aware Geometric Knowledge. We report results for the edge-aware geometric knowledge setting. To quantify the privileged information, we set the quantity $(|\mathcal{E}| - |\mathcal{E}'|)/|\mathcal{E}'|$, called *privileged information ratio* (PIR), as 0.5. As shown in Tab. 1, all variants of GKD outperform other KD baselines on both datasets, and significantly exceeds both Student and Teacher models. Further, GKD and its variants rival, if not surpass, the Oracle model. In other words, the student model trained using GKD could use far less graph topological information to achieve very close performance to competitors that are aware of the full graph topology during inference. Furthermore, the parametric PGKD performs better than its non-parametric counterparts in most cases, and GKD-R is the most effective non-parametric method in general. Despite that, GKD-G and GKD-S are also effective while being simpler. We presume that the performance variation of different GKD realizations stem from the different geometric property governed by the feature of datasets.

Node-Aware Geometric Knowledge. We further investigate on the node-aware geometric knowledge setting where the teacher model has access to more labeled nodes and their relations with the rest nodes. We set the PIR w.r.t. labeled nodes, defined as $(|\mathcal{V}_{train}| - |\mathcal{V}'_{train}|)/|\mathcal{V}_{train}|$, to 0.5. A unique challenge of this setting compared to the edge-aware counterpart is that, apart from graph topological information, the student model has less labeled training samples. As we can see from Tab. 2. The proposed GKD and its variants again consistently outperform KD baselines throughout all the cases, surpasses both Student and Teacher models, and are even as competitive as Oracle.

Larger Dataset. Table 3 presents results on a large graph, i.e., OGBN-Arxiv. We use the same PIR setting as citation networks, and choose the best variant of GKD to report in the table. Since the space complexity for GKD is $O(n^2)$, we randomly draw a mini-batch of nodes for computing the distillation loss in practice. Note that the loss function is unbiased as long as all nodes are evenly covered. It could also be seamlessly integrated with the original mini-batch method (by sampling ego-graphs) used for training large graphs without further modification. Again, we found our methods consistently outperform Teacher and Student models, and are close to the performance of the Oracle model, which suggests the effectiveness of GKD in large graphs.

Performance Variation with Privileged Ratio. The results with respect to varying privileged (edge-aware and node-aware) information ratio are given respectively in Fig. 2 and Fig. 3. The performance of Oracle model is invariant as it is trained and tested on the same (complete) graph. In general, for Teacher model, Student model, and vanilla KD, their performance drops with increasing PIR quantifying the information loss. In contrast, our method is significantly more robust, only showing slight performance deterioration, exceeding the Teacher model, and approaching the Oracle model. Besides, we find an interesting phenomenon that in the edge-aware setting on Pubmed dataset, the performance of Teacher model is the worst, presumably because that the Teacher is trained using

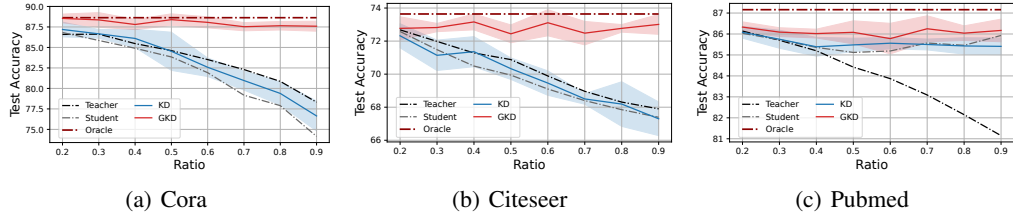


Figure 2: Performance variation with increasing PIR for the edge-aware knowledge setting.

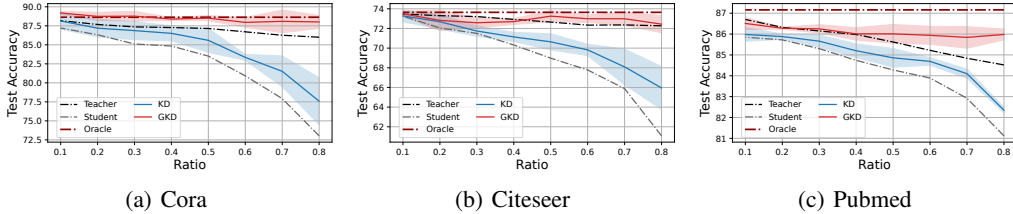


Figure 3: Performance variation with increasing PIR for the node-aware knowledge setting.

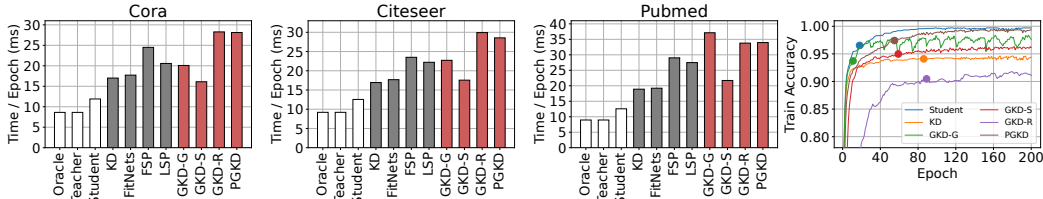


Figure 4: (Left three panels) Training time per epoch (ms) for GKD and baselines on citation networks. (Right panel) Convergence curves of different methods on Cora, where the circle denotes the epoch when the best validation accuracy has been reached.

fully observed graph, and may perform poorly once the privileged part of graph topology becomes unavailable at test time.

5.2 Scalability Test

Training Time. We report the the training time per epoch of different methods in the left three panels of Fig. 4, where we use the whole graph for training on Cora and Citeseer, and set the batch size as 5,000 for Pubmed. While the computation complexity for distillation loss of GKD (in both non-parametric and parametric cases) is $O(dn^2)$, we find that in practice their training time is not significantly worse than other KD baselines. In specific, all variants of GKD take less than two times of the training time of vanilla KD while yielding better performance, and the simplest GKD variant using Sigmoid NHK is even more efficient than baselines in some cases. It is also worth mentioning that the distilled student models are equally efficient by using sparser graph structure (in edge-aware setting) or smaller graph (in node-aware setting), which are suitable for being deployed in latency-constrained scenarios.

Convergence Speed. We also compare the convergence speed of different variants of GKD and other methods in the right panel of Fig. 4, where we use the same model architecture and optimizer for different methods and finetune other hyper-parameters to ensure fair comparison. Since the loss function is different for different methods, we report the convergence of training accuracy. As shown by the figure, GKD variants using Sigmoid and Gaussian NHKs can converge as fast as the vanilla KD. While GKD-R and PGKD in general take more epochs to converge, they can converge within 200 epochs (which is the default setting recommended in [28]) and the best validation accuracy is achieved within the first 100 epochs. We also find that the EM-style algorithm used for training PGKD does not cost too much extra epochs for convergence than the non-parametric GKD which is reasonable since the learnable mapping g_ϕ used in Eqn. (22) is an independent module that is not involved in GNN’s feed-forward computation.

	Oracle	Teacher	Student	GKD-G	GKD-S	GKD-R	PGKD
Offline	88.63 ± 0.48	84.61 ± 0.37	83.84 ± 1.32	87.68 ± 1.07	88.01 ± 0.79	88.48 ± 0.59	88.41 ± 0.62
Online	88.63 ± 0.48	84.61 ± 0.37	83.84 ± 1.32	87.75 ± 0.65	87.63 ± 0.65	88.28 ± 0.80	88.50 ± 0.33

Table 4: Comparison of offline and online distillation on Cora in edge-aware setting.

5.3 Other Settings

Setting	Teacher	Student	KD	GKD
Compression		SGC 85.93 ± 0.17	SGC 86.32 ± 0.32	SGC 87.15 ± 0.85
	GCN-64 88.76 ± 0.34	GCN-8 84.52 ± 1.34	GCN-8 87.50 ± 1.04	GCN-8 88.30 ± 0.46
		GCN-16 87.24 ± 0.43	GCN-16 88.09 ± 0.79	GCN-16 88.62 ± 0.50
Self-Distil		GCN-32 88.63 ± 0.48	GCN-32 88.98 ± 0.34	GCN-32 89.23 ± 0.52
		GCN-16 87.24 ± 0.43	GCN-16 87.62 ± 0.52	GCN-16 88.56 ± 0.40

Table 5: Node classification accuracy on Cora in settings: 1) model compression; 2) self-distillation.

Model Compression. We report the performance of GKD in the conventional model compression setting [22] where the teacher and student are different-sized GNN models. In this setting, we train and test both teacher and student models on the complete graph. We use GCN as the backbone for teacher with a relatively large hidden size 64, and use SGC or GCN (with hidden size 8 and 16) as the student model. We report the best result among all variants of GKD. As shown in the first section of Tab. 5, our method achieves notable improvements over the student model, rendering it as a useful KD approach for model compression.

Self-Distillation. We further report results for the setting of *self-distillation* [15; 37], which is a special case of KD when the teacher’s and student’s architectures are identical, often used for refining their own performance. The results as shown in Tab. 5 validate that GKD could also be used to effectively boost GNN’s own performance.

Online Distillation. Table. 4 shows the performance of different variants of GKD for online distillation where both the teacher model and the student model are trained in an end-to-end manner, in contrast to offline distillation where the teacher model is pre-trained. The results demonstrate the potential usage of GKD in this setting.

6 Conclusion, Current Limitations and Future Works

This paper formalizes the problem of graph topological knowledge transfer for GNNs. We investigate on the implication of heat kernel in GNNs and propose the novel notion of neural heat kernel. We leverage it to characterize the geometric property of the underlying manifold for graphs, and propose the framework of geometric knowledge distillation to transfer geometric knowledge from a teacher GNN model to a student GNN. Experimental results validate the effectiveness of our approach in various practical settings.

Despite that the proposed GKD is effective in various tasks and possesses decent training efficiency in practice, its theoretical space and time complexities are $O(n^2)$ and $O(dn^2)$ and the parametric instantiation may take some extra time to converge compared to the pure non-KD counterpart. The algorithmic complexity can be reduced by using mini-batch training, and there also exist ways to reduce the overhead such as pre-computing teacher’s NHK matrix or using low-rank approximation. Finally, we do not foresee any direct negative societal impacts of this work.

Acknowledgement

This work was partly supported by National Key Research and Development Program of China (2020AAA0107600), National Natural Science Foundation of China (61972250, 72061127003), and Shanghai Municipal Science and Technology (Major) Project (22511105100, 2021SHZDZX0102).

References

- [1] Jimmy Ba and Rich Caruana. Do deep nets really need to be deep? *NeurIPS*, 27, 2014.
- [2] Nicole Berline, Ezra Getzler, and Michele Vergne. *Heat kernels and Dirac operators*. Springer Science & Business Media, 2003.
- [3] Cristian Bodnar, Francesco Di Giovanni, Benjamin Paul Chamberlain, Pietro Liò, and Michael M Bronstein. Neural sheaf diffusion: A topological perspective on heterophily and oversmoothing in gnns. *arXiv preprint arXiv:2202.04579*, 2022.
- [4] Michael M Bronstein, Joan Bruna, Taco Cohen, and Petar Veličković. Geometric deep learning: Grids, groups, graphs, geodesics, and gauges. *arXiv preprint arXiv:2104.13478*, 2021.
- [5] Michael M Bronstein, Joan Bruna, Yann LeCun, Arthur Szlam, and Pierre Vandergheynst. Geometric deep learning: going beyond euclidean data. *IEEE Signal Processing Magazine*, 2017.
- [6] John Rozier Cannon. *The one-dimensional heat equation*. Number 23. Cambridge University Press, 1984.
- [7] Benjamin Chamberlain, James Rowbottom, Davide Eynard, Francesco Di Giovanni, Xiaowen Dong, and Michael Bronstein. Beltrami flow and neural diffusion on graphs. *NeurIPS*, 2021.
- [8] Benjamin Paul Chamberlain, James Rowbottom, Maria Gorinova, Stefan Webb, Emanuele Rossi, and Michael M Bronstein. Grand: Graph neural diffusion. *ICML*, 2021.
- [9] Yuzhao Chen, Yatao Bian, Xi Xiao, Yu Rong, Tingyang Xu, and Junzhou Huang. On self-distilling graph neural network. *arXiv preprint arXiv:2011.02255*, 2020.
- [10] Youngmin Cho and Lawrence Saul. Kernel methods for deep learning. *NeurIPS*, 22:342–350, 2009.
- [11] Fan RK Chung and Fan Chung Graham. *Spectral graph theory*. Number 92. American Mathematical Soc., 1997.
- [12] Francesco Di Giovanni, James Rowbottom, Benjamin P Chamberlain, Thomas Markovich, and Michael M Bronstein. Graph neural networks as gradient flows. *arXiv preprint arXiv:2206.10991*, 2022.
- [13] Moshe Eliasof, Eldad Haber, and Eran Treister. Pde-gcn: Novel architectures for graph neural networks motivated by partial differential equations. *Advances in Neural Information Processing Systems*, 34:3836–3849, 2021.
- [14] Matthew Fahrback, Gramoz Goranci, Richard Peng, Sushant Sachdeva, and Chi Wang. Faster graph embeddings via coarsening. In *ICML*, 2020.
- [15] Tommaso Furlanello, Zachary Lipton, Michael Tschannen, Laurent Itti, and Anima Anandkumar. Born again neural networks. In *International Conference on Machine Learning*, pages 1607–1616. PMLR, 2018.
- [16] Vikas K. Garg, Stefanie Jegelka, and Tommi S. Jaakkola. Generalization and representational limits of graph neural networks. In *ICML*, pages 3419–3430, 2020.
- [17] Jianping Gou, Baosheng Yu, Stephen J Maybank, and Dacheng Tao. Knowledge distillation: A survey. *International Journal of Computer Vision*, 129(6):1789–1819, 2021.
- [18] Alexander Grigoryan. *Heat kernel and analysis on manifolds*, volume 47. American Mathematical Soc., 2009.
- [19] Alexander Grigor’yan. Estimates of heat kernels on riemannian manifolds. *London Math. Soc. Lecture Note Ser.*, 273:140–225, 1999.
- [20] William L Hamilton, Rex Ying, and Jure Leskovec. Inductive representation learning on large graphs. In *NeurIPS*, pages 1025–1035, 2017.

- [21] Byeongho Heo, Jeeseo Kim, Sangdoon Yun, Hyojin Park, Nojun Kwak, and Jin Young Choi. A comprehensive overhaul of feature distillation. In *ICCV*, pages 1921–1930, 2019.
- [22] Geoffrey Hinton, Oriol Vinyals, and Jeff Dean. Distilling the knowledge in a neural network. *arXiv preprint arXiv:1503.02531*, 2015.
- [23] Weihua Hu, Matthias Fey, Marinka Zitnik, Yuxiao Dong, Hongyu Ren, Bowen Liu, Michele Catasta, and Jure Leskovec. Open graph benchmark: Datasets for machine learning on graphs. *NeurIPS*, 33:22118–22133, 2020.
- [24] Yu Jin, Andreas Loukas, and Joseph JaJa. Graph coarsening with preserved spectral properties. In *AISTATS*, 2020.
- [25] Matthias Keller and Daniel Lenz. Unbounded laplacians on graphs: basic spectral properties and the heat equation. *Mathematical Modelling of Natural Phenomena*, 5(4):198–224, 2010.
- [26] Jangho Kim, SeongUk Park, and Nojun Kwak. Paraphrasing complex network: Network compression via factor transfer. *Advances in neural information processing systems*, 31, 2018.
- [27] Diederik P. Kingma and Max Welling. Auto-encoding variational bayes. In *International Conference on Learning Representations*, 2014.
- [28] Thomas N Kipf and Max Welling. Semi-supervised classification with graph convolutional networks. *arXiv preprint arXiv:1609.02907*, 2016.
- [29] Johannes Klicpera, Aleksandar Bojchevski, and Stephan Günnemann. Predict then propagate: Graph neural networks meet personalized pagerank. *arXiv preprint arXiv:1810.05997*, 2018.
- [30] Johannes Klicpera, Stefan Weißenberger, and Stephan Günnemann. Diffusion improves graph learning. *arXiv preprint arXiv:1911.05485*, 2019.
- [31] Kyle Kloster and David F Gleich. Heat kernel based community detection. In *KDD*, pages 1386–1395, 2014.
- [32] Zenan Li, Qitian Wu, Fan Nie, and Junchi Yan. Graphde: A generative framework for debiased learning and out-of-distribution detection on graphs. In *Advances in Neural Information Processing Systems*, 2022.
- [33] David Lopez-Paz, Léon Bottou, Bernhard Schölkopf, and Vladimir Vapnik. Unifying distillation and privileged information. *ICLR*, 2016.
- [34] Hao Ma, Dengyong Zhou, Chao Liu, Michael R. Lyu, and Irwin King. Recommender systems with social regularization. In *International Conference on Web Search and Web Data Mining*, pages 287–296, 2011.
- [35] Andrew Kachites McCallum, Kamal Nigam, Jason Rennie, and Kristie Seymore. Automating the construction of internet portals with machine learning. *Information Retrieval*, 2000.
- [36] Georgi S Medvedev. The nonlinear heat equation on dense graphs and graph limits. *SIAM Journal on Mathematical Analysis*, 46(4):2743–2766, 2014.
- [37] Hossein Mobahi, Mehrdad Farajtabar, and Peter L Bartlett. Self-distillation amplifies regularization in hilbert space. *arXiv preprint arXiv:2002.05715*, 2020.
- [38] Federico Monti, Davide Boscaini, Jonathan Masci, Emanuele Rodola, Jan Svoboda, and Michael M Bronstein. Geometric deep learning on graphs and manifolds using mixture model cnns. In *CVPR*, pages 5115–5124, 2017.
- [39] Galileo Namata, Ben London, Lise Getoor, Bert Huang, and UMD EDU. Query-driven active surveying for collective classification. In *International Workshop on Mining and Learning with Graphs*, 2012.
- [40] Wonpyo Park, Dongju Kim, Yan Lu, and Minsu Cho. Relational knowledge distillation. In *Proceedings of the IEEE/CVF Conference on Computer Vision and Pattern Recognition*, pages 3967–3976, 2019.

- [41] Ali Rahimi, Benjamin Recht, et al. Random features for large-scale kernel machines. In *NIPS*.
- [42] Adriana Romero, Nicolas Ballas, Samira Ebrahimi Kahou, Antoine Chassang, Carlo Gatta, and Yoshua Bengio. Fitnets: Hints for thin deep nets. *arXiv preprint arXiv:1412.6550*, 2014.
- [43] Laurent Saloff-Coste. *Aspects of Sobolev-type inequalities*, volume 289. Cambridge University Press, 2002.
- [44] Prithviraj Sen, Galileo Namata, Mustafa Bilgic, Lise Getoor, Brian Gallagher, and Tina Eliassi-Rad. Collective classification in network data. *AI magazine*, 2008.
- [45] Matthew Thorpe, Tan Minh Nguyen, Hedi Xia, Thomas Strohmer, Andrea Bertozzi, Stanley Osher, and Bao Wang. Grand++: Graph neural diffusion with a source term. In *International Conference on Learning Representations*, 2021.
- [46] Jake Topping, Francesco Di Giovanni, Benjamin Paul Chamberlain, Xiaowen Dong, and Michael M Bronstein. Understanding over-squashing and bottlenecks on graphs via curvature. *arXiv preprint arXiv:2111.14522*, 2021.
- [47] Vladimir Vapnik, Rauf Izmailov, et al. Learning using privileged information: similarity control and knowledge transfer. *JMLR*, 16(1):2023–2049, 2015.
- [48] Dmitri V Vassilevich. Heat kernel expansion: user’s manual. *Physics reports*, 388(5-6):279–360, 2003.
- [49] Petar Veličković, Guillem Cucurull, Arantxa Casanova, Adriana Romero, Pietro Lio, and Yoshua Bengio. Graph attention networks. *ICLR*, 2018.
- [50] Shuai Wang, Kun Zhang, Le Wu, Haiping Ma, Richang Hong, and Meng Wang. Privileged graph distillation for cold start recommendation. *arXiv preprint arXiv:2105.14975*, 2021.
- [51] Yifei Wang, Yisen Wang, Jiansheng Yang, and Zhouchen Lin. Dissecting the diffusion process in linear graph convolutional networks. *NeurIPS*, 2021.
- [52] Andrew Gordon Wilson, Zhiting Hu, Ruslan Salakhutdinov, and Eric P Xing. Deep kernel learning. In *Artificial intelligence and statistics*, pages 370–378. PMLR, 2016.
- [53] Felix Wu, Amauri Souza, Tianyi Zhang, Christopher Fifty, Tao Yu, and Kilian Weinberger. Simplifying graph convolutional networks. In *ICML*, pages 6861–6871, 2019.
- [54] Qitian Wu, Chenxiao Yang, and Junchi Yan. Towards open-world feature extrapolation: An inductive graph learning approach. *Advances in Neural Information Processing Systems*, pages 19435–19447, 2021.
- [55] Qitian Wu, Hengrui Zhang, Junchi Yan, and David Wipf. Handling distribution shifts on graphs: An invariance perspective. In *International Conference on Learning Representations*, 2022.
- [56] Qitian Wu, Wentao Zhao, Zenan Li, David Wipf, and Junchi Yan. Nodeformer: A scalable graph structure learning transformer for node classification. In *Advances in Neural Information Processing Systems*, 2022.
- [57] Shu Wu, Mengqi Zhang, Xin Jiang, Xu Ke, and Liang Wang. Personalizing graph neural networks with attention mechanism for session-based recommendation. *TKDE*, 2019.
- [58] Bai Xiao, Edwin R Hancock, and Richard C Wilson. Geometric characterization and clustering of graphs using heat kernel embeddings. *Image and Vision Computing*, 28(6):1003–1021, 2010.
- [59] Keyulu Xu, Jingling Li, Mozhi Zhang, Simon S. Du, Ken-ichi Kawarabayashi, and Stefanie Jegelka. How neural networks extrapolate: From feedforward to graph neural networks. In *ICLR*, 2021.
- [60] Bencheng Yan, Chaokun Wang, Gaoyang Guo, and Yunkai Lou. Tinygnn: Learning efficient graph neural networks. In *KDD*, pages 1848–1856, 2020.

- [61] Cheng Yang, Jiawei Liu, and Chuan Shi. Extract the knowledge of graph neural networks and go beyond it: An effective knowledge distillation framework. In *WWW*, pages 1227–1237, 2021.
- [62] Chenxiao Yang, Junwei Pan, Xiaofeng Gao, Tingyu Jiang, Dapeng Liu, and Guihai Chen. Cross-task knowledge distillation in multi-task recommendation. *AAAI*, 2022.
- [63] Yiding Yang, Jiayan Qiu, Mingli Song, Dacheng Tao, and Xinchao Wang. Distilling knowledge from graph convolutional networks. In *CVPR*, 2020.
- [64] Junho Yim, Donggyu Joo, Jihoon Bae, and Junmo Kim. A gift from knowledge distillation: Fast optimization, network minimization and transfer learning. In *CVPR*, 2017.
- [65] Shan You, Chang Xu, Chao Xu, and Dacheng Tao. Learning from multiple teacher networks. In *Proceedings of the 23rd ACM SIGKDD International Conference on Knowledge Discovery and Data Mining*, pages 1285–1294, 2017.
- [66] Sergey Zagoruyko and Nikos Komodakis. Paying more attention to attention: Improving the performance of convolutional neural networks via attention transfer. *ICLR*, 2017.
- [67] Jiawei Zhang, Haopeng Zhang, Congying Xia, and Li Sun. Graph-bert: Only attention is needed for learning graph representations. *CoRR*, abs/2001.05140, 2020.
- [68] Ke Zhang, Carl Yang, Xiaoxiao Li, Lichao Sun, and Siu Ming Yiu. Subgraph federated learning with missing neighbor generation. *NeurIPS*, 34, 2021.
- [69] Shichang Zhang, Yozen Liu, Yizhou Sun, and Neil Shah. Graph-less neural networks: Teaching old mlps new tricks via distillation. *arXiv preprint arXiv:2110.08727*, 2021.

A Proof for Theorem 1

Suppose (\mathcal{M}, μ) is the base manifold of dimension n with respect to graph \mathcal{G} and GNN model f_θ , and $\Delta_\mu(\mathcal{G}, f_\theta)$ is the associated weighted Laplace operator with respect to \mathcal{G} and f_θ (in the following shortened as Δ_μ). We leverage a Sobolev inequality on manifolds as Lemma 1.

Lemma 1. [43] *Let x be a function from the local Sobolev space $\mathcal{W}_{loc}^{2\sigma}(\mathcal{M})$ for a positive integer $\sigma > n/4$. Then, for any relatively compact open set $\Omega \subset \mathcal{M}$ and any set $K \Subset \Omega$, there is a constant C such that*

$$\sup_K |x| \leq C \|x\|_{\mathcal{W}^{2\sigma}(\Omega)}. \quad (24)$$

where the norm $\|\cdot\|_{\mathcal{W}^{2\sigma}}$ is defined as

$$\|x\|_{\mathcal{W}^{2\sigma}}^2 = \sum_{l=0}^k \|\Delta_\mu^l x\|_{L^2}^2 \quad (25)$$

Suppose σ is the smallest integer larger than $n/4$, and $\mathbf{P}_t = e^{-t\mathcal{L}}$ is the heat kernel semigroup, where $\mathcal{L} = -\Delta_\mu|_{W_0^2}$ is the Dirichlet Laplace operator for the base manifold regarding graph \mathcal{G} and GNN model f_θ , we have the following lemma.

Lemma 2. *For any function $x \in L^2(\mathcal{M})$, $t > 0$, and set $K \Subset \mathcal{M}$, it holds that*

$$\sup_K |\mathbf{P}_t x| \leq C (1 + t^{-\sigma}) \|x\|_{L^2(\mathcal{M})}, \quad (26)$$

where C is a constant depending on K, \mathbf{g}, μ, n .

Proof. Suppose $\{E_\lambda\}$ is the spectral resolution of the Dirichlet operator \mathcal{L} for the base manifold. Consider the function $\Phi(\lambda) = \lambda^k e^{-t\lambda}$, where $t > 0$ and $k \in \mathbb{Z}^+$. We have

$$\mathcal{L}^k e^{-t\mathcal{L}} = \int_0^\infty \Phi(\lambda) dE_\lambda \quad (27)$$

Since $\Phi(\lambda)$ is bounded on $[0, +\infty)$, $\mathcal{L}^k e^{-t\mathcal{L}}$ is also bounded, and hence we have $\mathcal{L}^k (e^{-t\mathcal{L}} x) \in L^2(\mathcal{M})$. By noticing that the function $\lambda \mapsto \lambda^k e^{-t\lambda}$ takes its maximal value at $\lambda = k/t$, we have, for any $x \in L^2$,

$$\begin{aligned} \|\Delta_\mu^k \mathbf{P}_t x\|_{L^2} &= \|\mathcal{L}^k e^{-t\mathcal{L}} x\|_{L^2} \\ &= \left(\int_0^\infty (\lambda^k e^{-t\lambda})^2 d\|E_\lambda x\|_{L^2}^2 \right)^{1/2} \\ &\leq \sup_{\lambda \geq 0} (\lambda^k e^{-t\lambda}) \left(\int_0^\infty d\|E_\lambda x\|_{L^2}^2 \right)^{1/2} \\ &= \left(\frac{k}{t} \right)^k e^{-k} \|x\|_{L^2}. \end{aligned} \quad (28)$$

Using the definition of $\|\cdot\|_{\mathcal{W}^{2\sigma}}$ in Eqn. (25) and the result of Eqn. (28), we obtain

$$\begin{aligned} \|\mathbf{P}_t x\|_{\mathcal{W}^{2\sigma}} &= \sum_{k=0}^\sigma \left(\frac{k}{t} \right)^k e^{-k} \|x\|_{L^2} \\ &\leq C \left(1 + \sum_{k=1}^\sigma \left(\frac{k}{t} \right)^k e^{-k} \right) \|x\|_{L^2} \\ &\leq C' (1 + t^{-\sigma}) \|x\|_{L^2}. \end{aligned} \quad (29)$$

Substituting $\mathbf{P}_t x$ into Lemma. 1 and using the result of Eqn. 29 yields Eqn. 26, and thus completes the proof. \square

Consider the following equivalent expressions describing heat diffusion and feature propagation respectively,

$$\mathbf{H}^{(l+1)} = f_\theta(\mathbf{H}^{(l)}, \mathcal{G}), \quad \mathbf{X}(t + \tau) = e^{-\tau\Delta(f_\theta, \mathcal{G})}\mathbf{X}(t) \quad (30)$$

where τ is a constant dependent on f_θ and l . We can rewrite the single-layer NHK as a function p_{τ, v_i} such that for any $v_j \in \mathcal{V}$ (or equivalently $v_j \in \mathcal{M}$)

$$p_{\tau, v_i}(v_j) = \kappa_\theta^{(l)}(v_i, v_j). \quad (31)$$

We define $g : \mathcal{V} \rightarrow \mathbb{R}^d$ as a function that outputs the feature of a node in l -th layer, which is clearly Lebesgue integrable by thinking of nodes embedded on the manifold, i.e., $g \in L^2(\mathcal{M})$.

Proof for the existence of unique single-layer NHK boils down to proof that for any $v_i \in \mathcal{M}$, $l > 0$ (i.e., $\tau > 0$), there exists a unique function $p_{\tau, v_i} \in L^2(\mathcal{M})$ such that, for all g_θ ,

$$\mathbf{P}_\tau g_\theta(v_i) = \int_{v_j} p_{\tau, v_i} g_\theta(v_j) dv_j. \quad (32)$$

Fix a relatively compact set $K \Subset \mathcal{M}$. By Lemma 2, for all $\tau > 0$ and $g_\theta \in L^2(\mathcal{M})$, the function $\mathbf{P}_\tau g_\theta(v_i)$ admits the estimate

$$|\mathbf{P}_\tau g_\theta(v_i)| \leq C(1 + \tau^{-\sigma}) \|g_\theta(v_i)\|_{L^2(\mathcal{M})}. \quad (33)$$

Therefore, for fixed l and GNN model f_θ , the mapping $g_\theta \mapsto \mathbf{P}_\tau g_\theta$ is a bounded linear functional on $L^2(\mathcal{M})$. By the Riesz representation theorem, there exists a function $p_{\tau, v_i} \in L^2(\mathcal{M})$ such that

$$\mathbf{P}_\tau g_\theta = (p_{\tau, v_i}, g_\theta)_{L^2} \quad \text{for all } g_\theta \in L^2(\mathcal{M}), \quad (34)$$

where $(\cdot, \cdot)_{L^2}$ denotes inner product in L^2 , whence Eqn. (32) follows. The uniqueness of p_{τ, v_i} is evident from Eqn. (32) since for any point $v_i \in \mathcal{M}$ there is a compact set K containing v_i , the function $p_{\tau, v}$ is defined for all $\tau > 0$ and $v \in \mathcal{M}$.

B Proof for Theorem 2

Lemma 3. For all $v_i, v_j \in \mathcal{M}$ and $t > 0$, the inner product $(p_{s, x}, p_{t-s, y})$ does not depend on $s \in (0, t]$.

Proof. Using $\mathbf{P}_{t+s} = \mathbf{P}_s \mathbf{P}_t$ (by the definition of \mathbf{P}_t), Eqn. (34), and the symmetry of \mathbf{P}_t , we obtain that for all $v \in \mathcal{M}$, $t, s > 0$, and $g_\theta \in L^2(\mathcal{M})$, it holds that

$$\begin{aligned} \mathbf{P}_{t+s} g_\theta(v_i) &= \mathbf{P}_s (\mathbf{P}_t g_\theta)(v_i) \\ &= (\mathbf{P}_{s, v_i}, \mathbf{P}_t g_\theta) = (\mathbf{P}_t \mathbf{P}_{s, v_i}, g_\theta) \\ &= \int_{\mathcal{M}} \mathbf{P}_t \mathbf{P}_{s, v_i}(z) g_\theta(v_j) d\mu(v_j) \\ &= \int_{\mathcal{M}} (\mathbf{P}_{t, v_j}, \mathbf{P}_{s, v_i}) g_\theta(v_j) d\mu(v_j), \end{aligned} \quad (35)$$

□

Lemma 3 implies that, for all $v_i, v_j \in \mathcal{M}$ and $0 < s \leq t$

$$p_t(v_i, v_k) = (p_{s, v_i}, p_{t-s, v_k}). \quad (36)$$

Hence, it holds that

$$\begin{aligned} \int_{\mathcal{M}} p_t(v_i, v_j) p_s(v_j, v_k) d\mu(v_j) \\ = (p_t(v_i, \cdot), p_s(v_k, \cdot)) = p_{t+s}(v_i, v_k). \end{aligned} \quad (37)$$

By letting

$$s = \min\{\tau^{(l+1)}, \tau^{(l+2)}\}, \quad t = \max\{\tau^{(l+1)}, \tau^{(l+2)}\}, \quad (38)$$

we can rewrite Eqn. (37) as the expression of semigroup identity property of layer-wise NHK

$$\begin{aligned} \kappa_\theta(v_i, v_j, l \mapsto l+2) = \\ \sum_{v_k \in \mathcal{V}} \kappa_\theta^{(l+1)}(v_i, v_k) \kappa_\theta^{(l+2)}(v_k, v_j) d\mu(v_k). \end{aligned} \quad (39)$$

The proof also generalizes to the cross-layer case, inducing cross-layer NHK $\kappa_\theta(v_i, v_j, l \mapsto l+k)$.

C Proof for Theorem 3

Let $\{\varphi_k\}_{k=1}^{\infty}$ be an orthonormal basis of eigenfunctions of \mathcal{L} with an increasing sequence of non-negative eigenvalues $\{\lambda_k\}_{k=1}^{\infty}$, where $\lambda_k \rightarrow +\infty$. In consideration of

$$(p_{\tau, v_i}, \varphi_k)_{L^2} = P_{\tau} \varphi_k(v_i) = e^{-\tau \mathcal{L}} \varphi_k(v_i) = e^{-\tau \lambda_k} \varphi_k(v_i), \quad (40)$$

we have the following expansion of p_{t, v_i} by referring to results in literature [48]

$$p_{t, v_i} = \sum_k e^{-t \lambda_k} \varphi_k(v_i) \varphi_k. \quad (41)$$

Let T be the accumulated time interval from l -th layer to $(l+k)$ -th layer, in consideration of the equivalence shown in Eqn. (31), we could write Eqn. (41) as

$$\kappa_{\theta}(v_i, v_j, l \mapsto l+k) = \sum_{k'=0}^{\infty} e^{-\lambda_{k'} T} \varphi_{k'}(v_i)^{\top} \varphi_{k'}(v_j) \quad (42)$$

completing the proof.

D Justification for Parametric GKD

We justify parametric GKD from a variational inference perspective. From Eqn. (18), the forward GNN model f_{θ} defines a model distribution

$$p_{\theta}(\mathbf{H}^{(l)}, \mathbf{H}^{(l+k)}, \mathbf{K}) = p_{\theta}(\mathbf{H}^{(l)}) p_{\theta}(\mathbf{K} | \mathbf{H}^{(l)}) p_{\theta}(\mathbf{H}^{(l+k)} | \mathbf{K}, \mathbf{H}^{(l)}), \quad (43)$$

where $p_{\theta}(\mathbf{K} | \mathbf{H}^{(l)})$ is intractable, hindering the proceeding distillation. In this light, the variational inverse-NHK model κ_{ϕ}^{\dagger} is proposed with a variational distribution

$$q_{\phi}(\mathbf{H}^{(l)}, \mathbf{H}^{(l+k)}, \mathbf{K}) = q_{\phi}(\mathbf{H}^{(l+k)}) q_{\phi}(\mathbf{K} | \mathbf{H}^{(l+k)}) q_{\phi}(\mathbf{H}^{(l)} | \mathbf{H}^{(l+k)}, \mathbf{K}), \quad (44)$$

which has a tractable posterior $q_{\phi}(\mathbf{K} | \mathbf{H}^{(l+k)})$. Now, we justify our training scheme with iterative optimization for Eqn. (22) and (23) by the following proposition.

Proposition 1. *The optimization in Eqn. (22) and (23) essentially minimizes the following Kullback–Leibler (KL) divergence,*

$$\min_{\theta, \phi} \mathcal{D}_{kl} \left(q_{\phi}(\mathbf{K}, \mathbf{H}^{(l)}, \mathbf{H}^{(l+k)}) \parallel p_{\theta}(\mathbf{K}, \mathbf{H}^{(l)}, \mathbf{H}^{(l+k)}) \right), \quad (45)$$

and hence attempts to establish equivalence between two latent variable models p_{θ} and q_{ϕ} .

Proof. In the following, we use \mathbf{X} , \mathbf{Y} , \mathbf{K} to denote $\mathbf{H}^{(l)}$, $\mathbf{H}^{(l+k)}$, $\mathbf{K}(\mathcal{G}, l \mapsto l+k)$ for brevity. By definition in Section 4.2 we have a forward GNN model f_{θ} with the joint distribution of latent variables

$$p_{\theta}(\mathbf{X}, \mathbf{Y}, \mathbf{K}) = p_{\theta}(\mathbf{X}) \underbrace{p_{\theta}(\mathbf{K} | \mathbf{X})}_{\text{Intractable}} p_{\theta}(\mathbf{Y} | \mathbf{X}, \mathbf{K}), \quad (46)$$

and a variational inverse-NHK model κ_{ϕ}^{\dagger} with the joint distribution of latent variables

$$q_{\phi}(\mathbf{X}, \mathbf{Y}, \mathbf{K}) = q_{\phi}(\mathbf{Y}) \underbrace{q_{\phi}(\mathbf{K} | \mathbf{Y})}_{\text{Tractable}} q_{\phi}(\mathbf{X} | \mathbf{Y}, \mathbf{K}). \quad (47)$$

Based on these equations, we can write the KL-divergence between joint distributions of p_θ and q_ϕ as

$$\begin{aligned}
& \mathcal{D}_{\text{KL}}(q_\phi(\mathbf{X}, \mathbf{Y}, \mathbf{K}) \parallel p_\theta(\mathbf{X}, \mathbf{Y}, \mathbf{K})) \\
&= \iiint q_\phi(\mathbf{X}, \mathbf{Y}, \mathbf{K}) \log \frac{q_\phi(\mathbf{X}, \mathbf{Y}, \mathbf{K})}{p_\theta(\mathbf{X}, \mathbf{Y}, \mathbf{K})} d\mathbf{X}d\mathbf{Y}d\mathbf{K} \\
&= \mathbb{E}_{q_\phi(\mathbf{Y})} \left[\iint q_\phi(\mathbf{K}, \mathbf{X}|\mathbf{Y}) \log \frac{q_\phi(\mathbf{Y})q_\phi(\mathbf{K}, \mathbf{X}|\mathbf{Y})}{p_\theta(\mathbf{X}, \mathbf{Y}, \mathbf{K})} d\mathbf{X}d\mathbf{K} \right] \\
&= C' + \mathbb{E}_{q_\phi(\mathbf{Y})} \left[\iint q_\phi(\mathbf{K}, \mathbf{X}|\mathbf{Y}) \log \frac{q_\phi(\mathbf{K}, \mathbf{X}|\mathbf{Y})}{p_\theta(\mathbf{X}, \mathbf{Y}, \mathbf{K})} d\mathbf{X}d\mathbf{K} \right] \\
&= C' + \mathbb{E}_{q_\phi(\mathbf{Y})} \left[\mathbb{E}_{q_\phi(\mathbf{K}|\mathbf{Y})} \left[\int_{\mathbf{X}} q_\phi(\mathbf{X}|\mathbf{Y}, \mathbf{K}) \cdot \right. \right. \\
&\quad \left. \left. \log \frac{q_\phi(\mathbf{K}|\mathbf{Y})q_\phi(\mathbf{X}|\mathbf{Y}, \mathbf{K})}{p_\theta(\mathbf{X}, \mathbf{Y}, \mathbf{K})} d\mathbf{X} \right] \right] \\
&= C + \mathbb{E}_{q_\phi(\mathbf{Y})} \left[\mathbb{E}_{q_\phi(\mathbf{K}|\mathbf{Y})} \left[\int_{\mathbf{X}} q_\phi(\mathbf{X}|\mathbf{Y}, \mathbf{K}) \cdot \right. \right. \\
&\quad \left. \left. \log \frac{q_\phi(\mathbf{X}|\mathbf{Y}, \mathbf{K})}{p_\theta(\mathbf{X})p_\theta(\mathbf{Y}, \mathbf{K}|\mathbf{X})} d\mathbf{X} \right] \right] \\
&= C + \mathbb{E}_{q_\phi(\mathbf{Y})} \left[\mathbb{E}_{q_\phi(\mathbf{K}|\mathbf{Y})} \left[\underbrace{\mathcal{D}_{\text{KL}}(q_\phi(\mathbf{X}|\mathbf{Y}, \mathbf{K}) \parallel p_\theta(\mathbf{X}))}_{\text{Reconstruction Loss}} - \underbrace{\mathbb{E}_{q_\phi(\mathbf{X}|\mathbf{Y}, \mathbf{K})}[\log p_\theta(\mathbf{K}, \mathbf{Y}|\mathbf{X})]}_{\text{Prediction Loss}} \right] \right].
\end{aligned} \tag{48}$$

The first term C is a constant entropy with respect to q_ϕ . The second term is the KL-divergence between the variational posterior $q_\phi(\mathbf{X}|\mathbf{Y}, \mathbf{K})$ and the prior $p_\theta(\mathbf{X})$, which corresponds to the reconstruction loss in Eqn. (22) that attempts to learn a NHK that faithfully reflects the latent heat diffusion process describing the GNN feature propagation. The third term is negative log-likelihood, which corresponds to the prediction loss in Eqn. (23) that attempts to fit the dataset. Therefore, minimizing this KL-divergence amounts to the iterative optimization scheme of Eqn. (22) and (23). \square

E More Discussions on the Equivalence of Eqn.7

The equivalence of two equations in Eqn. 7 is based on recent works [8; 7; 51; 13; 12] that built connection between heat equation and GNN. The main result of these works is that by treating node features \mathbf{H} as signal \mathbf{X} (corresponding to $x(u, t)$ in heat equation Eqn. 2) on the graph, solving the heat equation with Euler scheme yields the formulation of a GNN layer. In other words, the GNN can be seen as the discretisations of the continuous diffusion process described by the heat equation. Correspondingly in Eqn. 7, the left equation is a general GNN layer (corresponding to discretized diffusion process), and the right equation is directly derived from Eqn. 7 (corresponding to continuous diffusion process).

Moreover, different definitions of Laplace-Beltrami operator Δ yield different GNNs. To be more specific, the simplest definition [8; 51] of Δ is by letting the gradient operator ∇ denote assigning each edge the difference of adjacent nodes' features, and the divergence operator ∇^* denote the summation of edge features obtained from last step. In this case, setting τ in Eqn. 2 as 1 yields SGC [53], and since it is being pointed out to be a potential cause of over-smoothing (which is one example to show the thermodynamic and geometric perspective is helpful for understanding GNNs), the authors in [51] further set smaller τ which yields DGC. Reinterpreting ∇^* as weighted sum of edge features yields GAT [8; 49] and any other GNN following the message passing scheme:

$$\text{MessagePassing}(\mathbf{h}_u, \mathcal{G}) = \sum_{v \in \mathcal{N}_u \cup u} s(\mathbf{h}_u, \mathbf{h}_v) \cdot \mathbf{h}_v, \tag{49}$$

where \mathcal{N}_u denotes neighbored nodes of u , and s denotes a parametric or non-parametric similarity score. The neighborhood summation could also be modified by changing the definition of ∇ , which yields GNNs based on learned structures (e.g., GDC [30]) and those with residual links (e.g., APPNP [29]). Further considering different discretization schemes (e.g., implicit scheme, multi-step schemes) yields different variants of GRAND [8; 7; 45] that are found more powerful than its simplification (presumably because it better matches the continuous diffusion process).

Unfortunately, not all GNNs have a simple form of Δ , and for some of them, whether there exists such Δ is an open research question. Therefore, we write the operator as $\Delta(f_\theta, \mathcal{G})$ to associate it with model f_θ and use equivalence in Eqn. 2 as an analytical assumption. The thermodynamic and geometric perspective used in the paper is fundamental and useful for studying the geometry property of GNNs, which has also been adopted by other works [3; 46; 51; 45; 8; 7]. For example, [3] attempts to explain heterophily and oversmoothing problems in GNNs by connecting GNNs to the heat equation defined by the sheaf Laplace-Beltrami operator $\Delta_{\mathcal{F}}$ and propose new GNN architectures based on the theory. Similarly, [45; 8; 7] propose new GNN architectures / rewiring methods from the same thermodynamic perspective, [51] explains over-smoothing issue of SGC based on the same equivalence of GNN and solve of heat equation, and [46] explains the over-squashing issue from a geometric perspective by analyzing the curvature. A common trait of these works is to draw analogies between GNNs and differential geometry / diffusion process to obtain meaningful theoretical results (ours: NHK as a characterization of GNN’s underlying geometry) that are used to guide implementation (ours: GKD for geometric knowledge transfer).

F Implementation Details

We present implementation details for our experiments for reproducibility. We implement our model as well as the baselines with Python 3.7, Pytorch 1.8 and Pytorch Geometric 1.7. All experiments are conducted on NVIDIA V100 with 16 GB memory. All parameters are initialized with Xavier initialization procedure. We train the model by Adam optimizer. Both teacher and student models are trained from scratch. For the main results reported in Tab. 1 and 2, we choose the backbone model as a 3-layer GCN with hidden size 32. In case that the graph is too large, we use mini-batch training (draw a mini-batch of nodes from the vertex set \mathcal{V}) for computing the distillation loss. All the experiments are repeated five times with random initialization.

F.1 Dataset Description

We choose three benchmark citation network datasets, i.e., Cora, Citeseer and Pubmed, and a large-scale network dataset OGB-Arxiv for node classification. For citation networks, we randomly split them into train/valid/test data according to the ratio 2:1:1. For OGB dataset, we follow the original splitting [23] for evaluation. The statistics of these datasets are summarized in Tab. 6.

Dataset	# Classes	# Nodes	# Edges	Metric
Cora [35]	7	2,485	5,069	Accuracy
Citeseer [44]	6	2,120	3,679	Accuracy
PubMed [39]	3	19,717	44,324	Accuracy
OGB-Arxiv [23]	40	169,343	1,166,243	Accuracy

Table 6: Statistics of Datasets.

F.2 Hyper-Parameter Tuning

For parameter tuning, we adopt grid search method to search for hyper-parameters on validation set. Since our model is only sensitive to α , one can use other more efficient searching strategies instead of grid search (e.g., coordinate descent, Bayesian optimization) to achieve very similar results. The descriptions for several hyper-parameters and their search spaces are shown in Tab. 7.

Notation	Description	Search Space
T	accumulated time interval	[0.25, 0.5, 1, 2, 4]
α	weight of the geometric distillation loss	[0.1, 0.3, 1.0, 3.0, 10.0, 30.0, 100.0, 300.0, 1000.0]
α_{kd}	weight of the label-based distillation loss	[0.0, 0.2, 0.4, 0.6, 0.8]
τ	temperature for label-based distillation loss	[0.25, 0.5, 1, 2, 4]
δ	weight for non-connection entries for distillation loss	[0.0, 0.1, 0.2, 0.4, 0.6, 0.8, 1, 2]
γ	learning rate	[0.0001, 0.001, 0.01, 0.1]

Table 7: Parameter searching space for GKD and its variants.

F.3 Implementation of non-parametric GKD

For Gauss-Weierstrass NHK in Eqn. (13), we treat the accumulated time interval T as a hyper-parameter that is consistent for all layers. For sigmoid NHK in Eqn. (13), we let $a = 1, b = 0$ and the NHK is simple dot-product with activation. For randomized NHK in Eqn. (16), we let $s = 2d$ for the random transformation matrix \mathbf{W} , and we use $\tanh(\cdot)$ as activation function for $\sigma(\cdot)$.

Algorithm 1: Training Algorithm for GKD.

Input: Complete graph $\tilde{\mathcal{G}}$ with labels $\tilde{\mathbf{Y}}$, partial graph \mathcal{G} with labels \mathbf{Y} , learning rate γ , initial parameters θ^*, θ .

Training Teacher GNN:

while *Not converged* **do**

Teacher model conducts feature propagation on $\tilde{\mathcal{G}}$
 Calculate $\mathcal{L}_{pre}(\hat{\mathbf{Y}}_{\theta^*}, \tilde{\mathbf{Y}})$ as in Eqn. (17)
 $\theta^* \leftarrow \theta^* - \gamma \nabla_{\theta^*} \mathcal{L}_{pre}(\hat{\mathbf{Y}}_{\theta^*}, \tilde{\mathbf{Y}})$

Save teacher model as f_{θ^*}

Training Student GNN:

Load teacher model f_{θ^*}

while *Not converged* **do**

Teacher model conducts feature propagation on $\tilde{\mathcal{G}}$
 Student model conducts feature propagation on \mathcal{G}
 Calculate \mathcal{L}_{pre} and \mathcal{L}_{dis} as in Eqn. (17)
 $\theta \leftarrow \theta - \gamma \nabla_{\theta} \mathcal{L}_{pre}(\hat{\mathbf{Y}}_{\theta}, \mathbf{Y}) + \frac{\alpha}{L} \sum_{l=1}^L \mathcal{L}_{dis}^{(l)}$

F.4 Implementation of parametric GKD

For the case of parametric GKD, we realize the non-linear mapping g_{ϕ} as a neural network one-layer feed-forward neural network with $\tanh(\cdot)$ activation, and set $s = 2d$, the same as the non-parametric setting. In case that the teacher model has larger hidden size than the student model, we follow standard approaches in feature-based knowledge distillation methods [21] and use independent mappings for teacher and student models that are customized for their own hidden sizes. We use an EM-style algorithm for training the student model as in Eqn. (22) and Eqn. (23). For variants of GKD+KD and PGKD+KD, we consider additional standard label-based distillation loss in [22] with respect to labeled nodes, inducing an additional hyper-parameter α_{kd} that controls its importance.

F.5 Descriptions and Implementations of Baselines

KD [22]: is the seminal work of knowledge distillation, which uses the predictions of the teacher model as soft labels to teach the student model.

FitNets [42]: is the representative work of feature-based knowledge distillation, using the intermediate layers of training instances to teach the student model.

FSP [64]: is a relation-based knowledge distillation method, using the Gram matrix between two intermediate layers to explore the relationships between different feature maps.

LSP [63]: is a knowledge distillation method for graph convolutional networks, which aims to match the local distribution (similarity with adjacent nodes) of teacher and student models.

Note that some of these baselines (FitNets and FSP) are originally designed specifically for computer vision tasks, we adapt them to the setting of graph neural networks with slight modifications. While FSP is designed for graph neural networks, its original formulation of distillation loss does not account for the difference of graph topology for teacher and student models. To make it compatible with the settings considered in this paper, we fix the definition of local structures with respect to either student or teacher graph topology, and choose the best result for report. We refer to the hyper-parameter settings in their papers and also finetune them on different datasets.

Algorithm 2: Training Algorithm for PGKD.

Input: Complete graph $\tilde{\mathcal{G}}$ with labels $\tilde{\mathbf{Y}}$, partial graph \mathcal{G} with labels \mathbf{Y} , learning rate γ_1 and γ_2 , initial parameters θ^* , θ , ϕ .

Training Teacher GNN:

while *Not converged* **do**

 Teacher model conducts feature propagation on $\tilde{\mathcal{G}}$

 Calculate $\mathcal{L}_{pre}(\hat{\mathbf{Y}}_{\theta^*}, \tilde{\mathbf{Y}})$ as in Eqn. (17)

$\theta^* \leftarrow \theta^* - \gamma_1 \nabla_{\theta^*} \mathcal{L}_{pre}(\hat{\mathbf{Y}}_{\theta^*}, \tilde{\mathbf{Y}})$

Save teacher model as f_{θ^*}

Training Student GNN:

Load teacher model f_{θ^*}

while *Not converged* **do**

 Teacher model conducts feature propagation on $\tilde{\mathcal{G}}$

Optimization for ϕ

 Student model conducts feature propagation on \mathcal{G}

 Calculate reconstruction loss \mathcal{L}_{rec} as in Eqn. (22)

$\phi \leftarrow \phi - \gamma_2 \nabla_{\phi} \mathcal{L}_{rec}$

Optimization for θ

 Calculate \mathcal{L}_{pre} and \mathcal{L}_{dis} as in Eqn. (23)

$\theta \leftarrow \theta - \gamma_1 \nabla_{\theta} (\mathcal{L}_{pre}(\hat{\mathbf{Y}}_{\theta^*}, \mathbf{Y}) + \alpha \mathcal{L}_{dis})$

G More Related Works

Knowledge Distillation. There are mainly four different types of distilling strategies [17], namely response-based KD [22] (which uses output layer of the teacher model to teach student), feature-based KD [42; 66; 21; 26] (which matches intermediate layers of teacher and student), relation-based KD [64; 65; 40; 62] (which aligns the relationship between different layers or samples), and graph-based KD [60; 63] (which considers the graph information or designed for GNN). For experiments, we choose representative method from each category as baselines. While these existing distillation strategies have shown remarkable success in distillation tasks such as model compression, they rarely (carefully) study the role of graph geometry in GNN iterations. For geometric knowledge transfer task, it is crucial to find a fundamental and principled way to track how graph topology affects the behavior of a specific GNN. Therefore, we first probe the intersection between KD and geometric learning, propose NHK to characterize geometric knowledge and propose different variants of GKD that are shown to be effective especially in the geometric knowledge transfer setting.

Generalization of GNNs. Recent advances shed lights on the generalization ability of GNNs from various perspectives, e.g., the in-distribution generalization error [16], extrapolation capability [59], out-of-distribution (OOD) generalization under distribution shifts [55] and the reliability against outliers and OOD testing data [32]. Our work can be seen a specific embodiment for GNN generalization w.r.t. topological domain transfer. Furthermore, there are some recent studies exploring learning under the varied data space between training and inference [54], using GNNs as an encoding and reasoning tool. GKD focuses on transferring across varied structural information and aims at compressing topological information for GNNs.